

THE 4TH INTERNATIONAL CONFERENCE ON ALUMINUM ALLOYS

SUPERPLASTIC BEHAVIOUR AND MICROSTRUCTURAL EVOLUTION IN AN Al-4wt%Mn ALLOY

N. Ridley, A.Hassani and F.J. Humphreys

University of Manchester/UMIST, Materials Science Centre, Grosvenor Street, Manchester M1 7HS, UK

Abstract

Studies of the superplastic deformation potential of an Al-4wt%Mn alloy produced by a powder route have been examined. Material which was received in the form of rod and sheet showed a microstructure consisting of heavily dislocated sub-grains containing a relatively large volume fraction of fine Al₆Mn dispersoids. The alloy showed a high resistance to static recrystallization. Testing under optimum conditions at constant strain rate led to tensile elongations >300%, but these could be further increased by control of the strain rate path. TEM studies showed that the low angle boundary sub-grain structure obtained on heating to the superplastic deformation temperature developed on straining into a fine grain microstructure containing high angle boundaries capable of sustaining grain boundary sliding.

Introduction

Previous studies on an Al-4wt%Mn alloy processed by a powder route showed that the material gave a tensile elongation of $\approx 90\%$ when tested at 500°C at a strain rate of $2.5 \times 10^{-3} \text{ s}^{-1}$ [1]. This moderately high elongation suggested that the alloy might exhibit significant superplastic (SP) behaviour if tested under more optimum conditions of temperature and strain rate.

The present investigation was carried out to determine whether the material was able to exhibit significant superplasticity and, if so, to identify the optimum deformation conditions and the way in which the microstructure evolved during SP deformation.

Experimental

The material was received from the British Petroleum Research International Centre (BPRI) in the form of 12.7mm diameter extruded rod and 2mm thick rolled sheet. The alloy had been

manufactured by a powder route, and after HIPping to 100% density was either extruded to rod or rolled at 400°C to sheet of 2mm thickness. The chemical analysis (wt%) of the alloy was Al-3.81Mn-0.10Si-0.07Fe-0.03Mg-0.01Ni-0.01Zn.

Investigation of the SP deformation potential was made using flat tensile specimens of 10mm gauge length and 5mm gauge width which were machined parallel to the rolling direction of the sheet. Testing was carried out using a three-zone split furnace attached to the cross-head of an Instron tensile machine which was interfaced with a microcomputer. Tensile testing to failure was carried out for a range of constant strain rates, and the strain hardening coefficient, n , was measured as a function of strain from the true stress-true strain data obtained from these tests. To study the effect of strain rate path on SP ductility and flow stress, various rapid strain rate tests to predetermined strains were also carried out, prior to deformation at optimum rates.

To supplement the studies of microstructural evolution during tensile testing, some compression tests were carried out on cylindrical specimens 25mm length and 12.5mm diameter. These were deformed at 450°C, 500°C and 550°C to a 50% reduction in height ($\epsilon = -0.69$) at a strain rate of $5 \times 10^{-4} \text{ s}^{-1}$, and then water quenched from temperature, prior to microstructural examination. Microstructural studies were carried out using optical microscopy, SEM and TEM. A computer programme was developed to obtain misorientations across grain/subgrain boundaries, from electron diffraction spot patterns.

Results and Discussion

Mechanical Behaviour

The relationship between flow stress and strain rate was examined using cross-head velocity cycling tests [2] for temperatures of 500°C, 550°C and 570°C. It can be seen in Figure 1a that there is a general increase in flow stress level with increasing temperature, and that at each temperature the logarithmic plot shows the sigmoidal form usually associated with SP materials. The slopes of the curves, which are equal to the strain rate sensitivities, or m values, are shown in Figure 1b. Maximum ' m ' values were obtained for the strain rate range 10^{-3} - 10^{-4} s^{-1} for the three temperatures. However, the maximum m values of ≈ 0.3 at 500°C were marginal for SP behaviour, but at 570°C ' m ' increased to > 0.5 .

Constant strain rate to failure tests were carried out at temperatures ranging from 450°C to 600°C, and the results are summarised in Figure 2. It can be seen for each strain rate that the tensile elongation passes through a maximum at $\approx 570^\circ\text{C}$, with the highest elongation of $\approx 330\%$ being observed for the lowest strain rate examined ($2.5 \times 10^{-4} \text{ s}^{-1}$).

True stress-true strain relationships are shown in Figure 3 for a strain rate of $5 \times 10^{-4} \text{ s}^{-1}$. For the temperatures examined, peak stress values were recorded for true strains of 0.4-0.6.

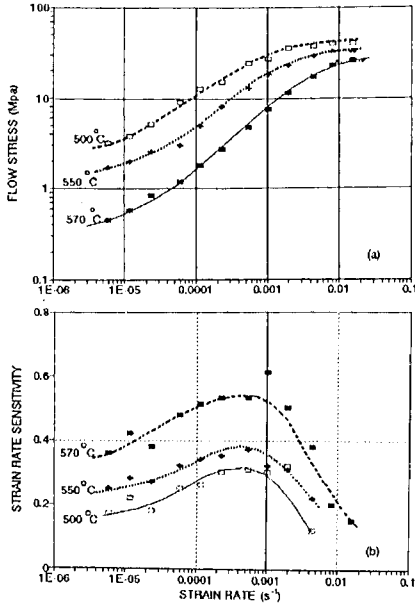


Fig.1 (a) Flow stress and (b) m values versus strain rate.

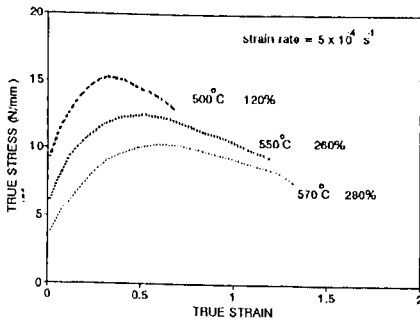


Fig.3 True stress vs true strain at various temperatures at $5 \times 10^{-4} \text{ s}^{-1}$.

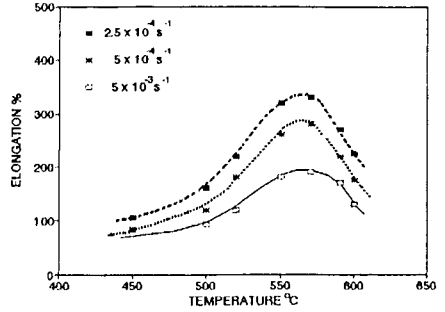


Fig.2 Elongation to failure as a function of temperature and strain rate.

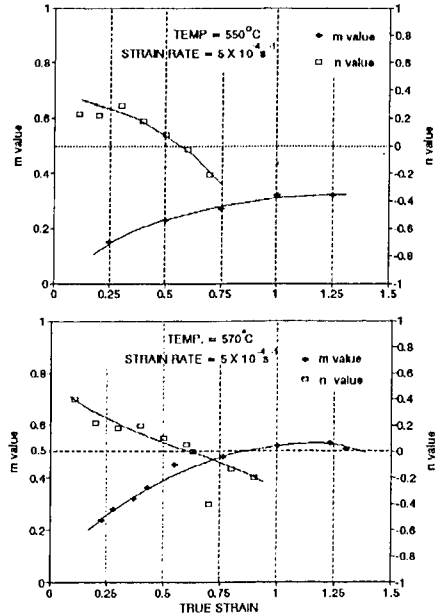


Fig.4 Variation of m and n with strain.

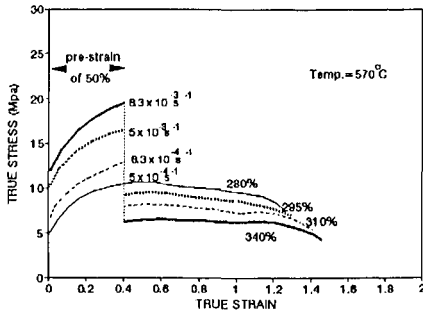


Fig.5 Effect of pre-strain rate on flow stress and strain to failure at $5 \times 10^{-4} \text{ s}^{-1}$.

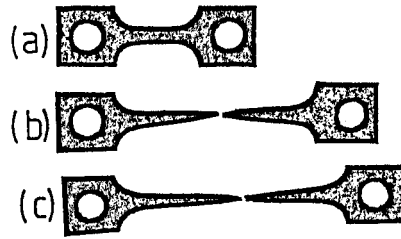


Fig.6 Profiles of tensile specimens (a) undeformed, (b) strained to failure at $5 \times 10^{-4} \text{ s}^{-1}$, 570°C , (c) pre-strained to 0.4 at $8.3 \times 10^{-3} \text{ s}^{-1}$ and strained to failure at $5 \times 10^{-4} \text{ s}^{-1}$, 570°C .

This is probably due to the onset of necking, but despite this the specimens were able to sustain appreciable strains to failure, particularly at 550°C and 570°C . Strain rate jump tests were carried out at 550°C and 570°C to examine the variation of m as a function of strain. It can be seen in Figure 4 that at both temperatures, the value of m is too low in the early stages of deformation to maintain substantial tensile stability.

It was first shown by Ash and Hamilton [3] that strain hardening could make a significant contribution to tensile stability for alloys in which the superplastic microstructure evolved by dynamic or strain-enhanced recrystallisation. For the present work, measured values of the strain hardening index, n , are superimposed on those of m in Figure 4. It can be seen that at the start of deformation, although the m values are low, the values of n are relatively high, and strain hardening will make a contribution to tensile flow stability. Nevertheless, at neither temperature is this sufficient to prevent the onset of necking (Fig.3). However, with increasing strain at 570°C the value of m is increasing and at the stage when $n > 0$, it is sufficiently high (> 0.3) to inhibit rapid neck propagation so leading to a significant tensile strains to failure. Figure 4 shows that the value of m continues to increase with increasing strain almost to the point of failure. Similar behaviour is apparent at 550°C , but at the stage when $n > 0$, the value of m is still < 0.3 . Surprisingly, this is sufficiently high to inhibit catastrophic failure and m continues to rise slowly throughout deformation to a value > 0.3 .

Previous studies have shown for alloys in which the SP microstructure evolves by strain-enhanced recrystallisation, that the application of a rapid pre-strain rate followed by deformation at a lower, near optimum, strain rate, can lead to a significant enhancement of superplastic ductility [4]. In the present study the effect of various rapid strain rates, applied for a pre-strain of 0.4 (50% elongation) are shown in Figure 5. It can be seen for the range of pre-strain rates examined that there are two important effects: the tensile strain to failure increases with increasing pre-strain rate, and the flow stress levels progressively decrease after

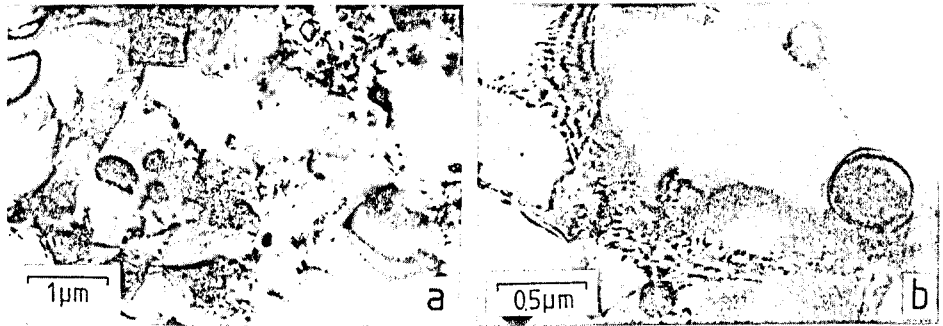


Fig.7 TEM (a) as-received material showing dislocated structure, (b) annealed 570°C for 60 minutes showing dislocations and sub-boundaries pinned by dispersoids.

pre-straining. Figure 6 shows the profiles of tensile specimens pulled to failure, with and without the application of a rapid pre-strain. Hence, the benefits of controlling the strain rate path are clearly demonstrated for this material.

Microstructural Examination

The particles in the as-received materials consist of Al_6Mn dispersoids of sub-micron dimensions and nanoscale aluminum oxide particles produced mainly during the powder processing [1]. TEM examination revealed a heavily dislocated substructure which showed a high resistance to static recrystallization (Figs.7a and b). In general, small particles, normally less than $1\mu m$ in diameter, retard recrystallization by pinning subgrain boundaries and restraining subgrain coalescence [5]. The pinning effect of Al_6Mn particles on sub-grain boundaries is clearly seen in Figure 7b. It has been proposed by Humphreys [6] that recrystallization is retarded if $F_v/d \geq 0.1\mu m^{-1}$, where F_v is the particle volume fraction and d the particle size. For the Al_6Mn dispersoids in the present material $F_v \approx 0.1$ and $d \approx 0.3\mu m$, thus fulfilling the condition predicted for the inhibition of recrystallization. The presence of fine aluminum oxide particles would enhance the pinning of subgrain boundaries. A dislocated substructure would also tend to be retained if the driving force for recrystallisation was reduced by hot working [7], which is consistent with the method of production of the alloy being investigated.

On straining at the optimum superplastic deformation temperature of 570°C, it was noted that the strain rate sensitivity, m , was initially low, and this would be expected if relatively few large angle boundaries capable of sustaining grain boundary sliding, were present. If the material is to exhibit superplastic behaviour it is necessary for the low angle boundaries to be converted to higher angle boundaries. The observation that m increases with increasing strain indicates that this is occurring, particularly at 570°C (Fig.4). However, in the early stages,

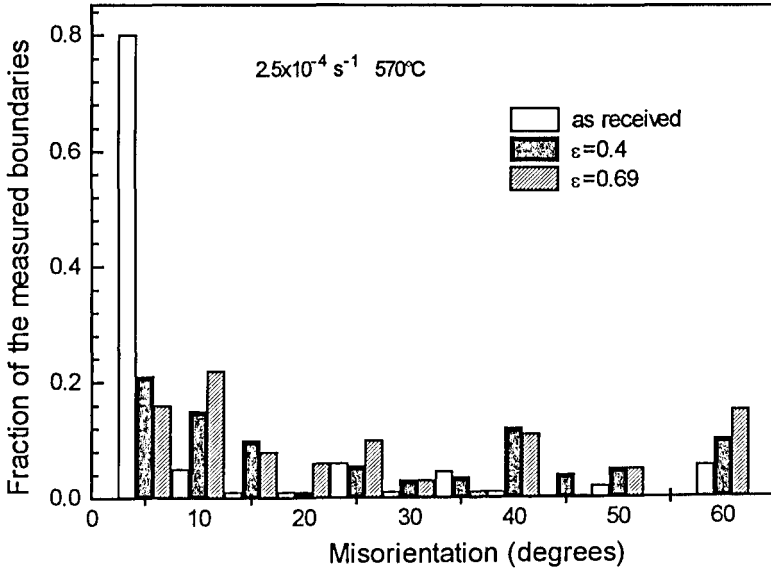


Fig.8 Effect of tensile deformation on boundary misorientation in sheet material.

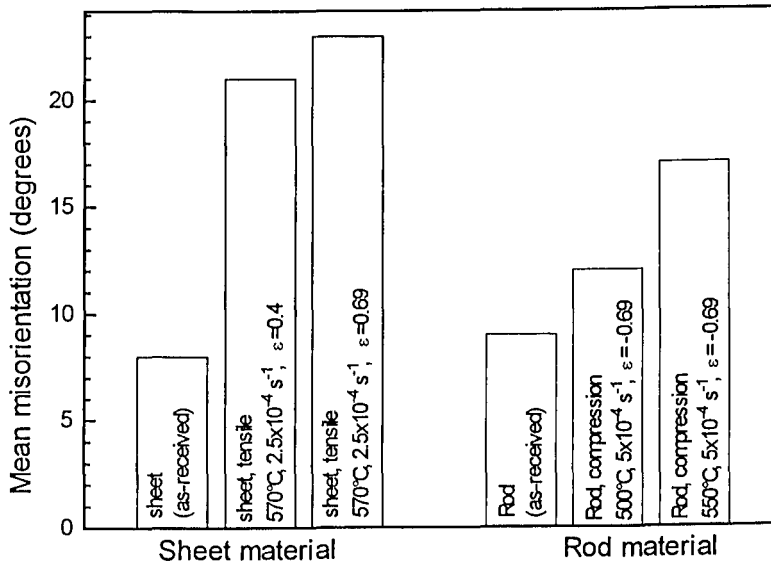


Fig.9 Mean values of boundary misorientation for specimens deformed in tension or compression.

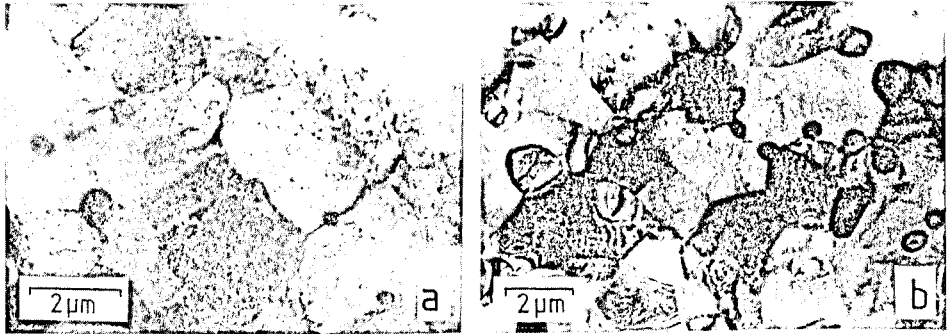


Fig.10 TEM of specimens deformed in tension showing (a) evidence of sub-grains and dislocations ($\epsilon=0.4$), (b) an almost fully recrystallized microstructure ($\epsilon=0.69$).

deformation must occur by intragranular slip involving the generation and movement of dislocations, and this would lead to the high initial rate of strain hardening (n), which is observed (Fig.4). If the dislocations are absorbed by sub-grain boundaries this would result in increasing misorientation across the boundaries, and eventually to a change in deformation mechanism from slip to grain boundary sliding. This change is consistent with the increasing in m and decrease in n observed (Fig.4).

Measurements of grain boundary misorientation have been made for the as-received material and for specimens deformed in both tension and compression, and the results are shown in Figs. 8 and 9. Figure 8 shows the distributions of misorientation in the as-received sheet and in tensile specimens deformed at 570°C to elongations of 50% and 100% ($\epsilon=0.4$ and 0.69, respectively). The as-received material shows mainly low angle boundaries with relatively few high angle boundaries. On deformation there is a progressive increase in the number of higher angle boundaries. The corresponding TEM microstructures are seen in Fig.10a and b. At a strain of 0.4 there is still evidence of dislocations and sub-grains in the microstructure (Fig.10a), but after a strain of 0.69 the material appears to be substantially recrystallized (Fig.10b).

The mean misorientations of boundaries are shown in Fig.9, both for the data in Fig.8, and also for the specimens deformed in compression. It can be seen that for compressive deformation at 500°C there is only a relatively small change in misorientation. At 550°C the changes are more marked, although less than those for tensile deformation at the optimum deformation temperature of 570°C. Recent work by Matsuki et al [8] has shown a similar mode of boundary misorientation evolution for a PM7475-0.7%Zr alloy deformed in tension at 520°C.

Conclusions

1. An Al-4wt%Mn alloy produced by a powder route and received in the form of rod and sheet showed a significant potential for SP deformation. Testing at constant strain rate under optimum conditions for SP tensile flow led to elongations >300%.
2. The as-received material had a microstructure consisting of heavily dislocated sub-grains with a relatively large volume fraction (≈ 0.1) of fine ($\approx 0.3\mu\text{m}$) Al_6Mn dispersoids, and also contained fine aluminium oxide particles. The material had a high resistance to static recrystallization.
3. On deformation at the optimum temperature, strain hardening made a significant contribution to the initial tensile stability while the strain rate hardening parameter, m , was increasing from its initially low value.
4. The application of a relatively rapid pre-strain rate led to an enhancement of tensile ductility, and to a fall in flow stress.
5. Measurement of boundary misorientations for specimens deformed in tension or compression showed that the initial low angle boundary sub-structure developed on straining into a fine grain microstructure with a high proportion of large angle boundaries capable of sustaining SP flow.

References

1. A. Basu, Ph.D. thesis, University of Manchester (1992).
2. W.A. Backofen, I.R. Turner and D.A. Avery, Trans. ASM, 57 (1964) 980.
3. B.A. Ash and C.H. Hamilton, Scripta Metall. 22 (1988) 277.
4. R. Amichi and N. Ridley, Proc. 5th Intl. Al-Li Conf., ed. T.H. Sanders and E.A. Starke (Birmingham, UK, MCEP, 1989) 159.
5. F.J. Humphreys, Met. Sci. 13 (1979) 136.
6. F.J. Humphreys, Acta Metall. 25 (1977) 1323.
7. F.J. Humphreys, W.S. Miller and M.R. Djazeb, Mater. Sci. Technol. 6 (1990) 1157.
8. K. Matsuki, H. Matsumoto and M. Tokizawa, Superplasticity in Advanced Materials, ed. S. Hori, M. Tokizane and N. Furushiro, (JSRS, Osaka, Japan, 1991) 551.